

Corrosion inhibition study of Aluminum alloy by using cerium compounds extracted from Egyptian monazite

Presented by

Amr Mohamed Mohamed Ahmed Shaltot M.Sc.(Chemistry), Ain-Shams University 2012

A Thesis submitted for Ph.D degree (Chemistry)

Chemistry Department
Faculty of Science
Ain Shams University

2019



Corrosion inhibition study of Aluminum alloy by using cerium compounds extracted from Egyptian monazite

Presented by Amr Mohamed Mohamed Ahmed Shaltot M.Sc. (Chemistry), Ain-Shams University 2012

A Thesis submitted for Ph.D degree (Chemistry)

Under the supervision of

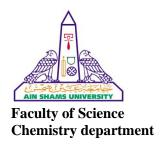
Prof.Dr. Sayed Sabet Abdel-Rehim Professor of physical chemistry Faculty of Science Ain Shams University

Prof.Dr. Hamdy Hassanien Hassan Professor of physical chemistry Faculty of Science Ain Shams University

Prof.Dr. Omneya Mohamed El Hussaini Professor of inorganic chemistry Deputy head of production sector for technical affairs Nuclear Materials Authority

Prof. Dr. Mohamed Abdel-Moniem Deyab Professor of physical chemistry Egyptian Petroleum Research Institute (EPRI)

2019



APPROVAL SHEET

Corrosion inhibition study of Aluminum alloy by using cerium compounds extracted from Egyptian monazite

Presented by Amr Mohamed Mohamed Ahmed Shaltot M.Sc. (Chemistry), Ain-Shams University 2012

A Thesis submitted for Ph.D degree (Chemistry)

NameSignature

Prof.Dr. Sayed Sabet Abdel-Rehim Professor of physical chemistry Faculty of Science Ain Shams University

Prof.Dr. Hamdy Hassanien Hassan Professor of physical chemistry Faculty of Science Ain Shams University

Prof.Dr. Omneya Mohamed El Hussaini Deputy head of production sector for technical affairs Nuclear Materials Authority

Prof.Dr. Mohamed Abdel-Moniem Deyab Professor of physical chemistry Egyptian Petroleum Research Institute (EPRI)

Head of Chemistry Department
Faculty of Science – Ain Shams University
Prof.Dr. Ibrahim Ali Badr

ACKNOWLEDGEMENT

First and foremost, all thanks and praise to *Allah*, the most mercifulfor giving meprosperity and strength to fulfill this work.

Special thanks and deep gratitude are devoted to *Prof. Dr. Sayed Sabet Abdel-Rehim* (Faculty of Science, Ain Shams University) for his supervision, generous guidance, great support, valuable advice and sincere help throughout this work.

I cannot thank enough *Prof. Dr. Omneya Mohamed El Hussaini* (Deputy head of production sector for technical affairs, Nuclear Materials Authority) for her input. I will be forever indebted for her constant guidance and scientific knowledge throughout my Ph.D. As a fellow supporter, I couldn't have asked for a better supervisor and fruitful discussions in all steps of this work.

I would like to thank *prof. Dr. Hamdy Hassanien Hassan* (Faculty of Science - Ain Shams University) for help and following up the details of this study.

Special gratitude and deep acknowledgements are to *Prof. Dr.* Mohamed Abdel-Moniem Deyab (Egyptian Petroleum Research Institute (EPRI)) for his valuable knowledge about the practical work and scientific information that has been essential during my Ph.D.

I would also like to thank. *Dr. Waleed Mahmmoud and Dr. Ahmed Abdel-Kareem* (Nuclear Materials Authority) for supplying the ore samples and for helping us to complete this work.

Deepest thanks for all the staff members and colleagues of Department, SEM lab. and the team work of XRD lab., Nuclear Materials Authority for encouragement and cooperation. Many thanks are to the staff members, head of Chemistry Department, and Dean of the Faculty of Science, Ain Shams University for their help in this work.

Many thanks to my mother, my son, all the family and the soul of my father.

Contents

		Page
Chap	eter 1: Introduction	1
1.1	Aluminum	1
1.2	The Corrosion Process	2
1.3	The methods used for corrosion protection measurements	6
1.4	Corrosion Inhibitors	9
1.5	The Surfactants	13
1.6	The Rare Earths	14
1.7	Literature Survey	21
1.8	Aim of the work	25
Chap	ter 2: Experimental	26
2.1	Chemicals and Reagents	26
2.2	Methodology	27
2.3	Part 1	28
2.4	Part 2	29
2.5	Part 3	30
2.6	Part 4	30
2.7	Part 5	32
2.9	Analytical Methods	35
2.10	Instruments	36
Chap	eter 3: Results and Discussion	37
Part	1: Inhibition of AA6061 in di-Sodium hydrogen phosphate by Surfactant	37
3.1.1	Effect of Surfactant Concentration (Polarization technique)	37
3.1.2	Impedance Measurements	44
3.1.3	Activation Energy	52
3.1.4	Adsorption Isotherm	54
Part	2: Inhibition of AA6061 in Sodium Chloride Solution by Surfactant	59

3.2.1	Effect of Surfactant Concentration (Polarization technique)	59
3.2.2	Impedance Measurements	65
3.2.3	Adsorption Isotherm	68
3.2.4	Effect of Temperature	71
3.2.5	Effect of Scan Rate	77
3.2.6	Chronoamperometry	80
Part 3	3: Inhibition of AA6061 in di-Sodium hydrogen phosphate by Cerium salts	87
3.3.1	Effect of Cerium salt concentration	87
3.3.2	Effect of Temperature	98
3.3.3	Effect of Immersion Time	102
3.3.4	Effect of Scan Rate	105
Part 4	4: Inhibition of AA6061 in Sodium Chloride Solution by Cerium salts	108
3.4.1	Effect of Cerium salt concentration	108
3.4.2	Effect of Temperature	123
3.4.3	Effect of Immersion Time	127
3.4.4	Effect of pH	130
Morp	hology	131
Part 5	5: Extrction of Cerium salts from Egyptian Monazite	134
3.5.1	Chemical treatment of monazite concentrates	134
3.5.2	Recovery Procedure	134
3.5.2.	4 Separation of Pure Cerium from the Prepared Monazite RE Cake	136
3.5.2	5 Optimization of the stripping process	140
3.5.2.	6 Technical working flowsheet	153
Conc	lusions	155
Refer	rences	159
Arabi	ic Summary	

List of Tables

Table	I	Page
1	The chemical composition of aluminum alloy 6061	1
2	The average rare earth content in % of the major rare earth mineral	16
3	Chemicals and reagents used in the experimental work	26
4	Factors affecting the solvent extraction of Ce	33
5	Factors affecting the stripping of Ce	34
6	The electrochemical parameters and the corresponding inhibition efficiency of AA6061 in 1 M Na ₂ HPO ₄ in the absence and presence of different concentrations of polysorbate 80 at different temperatures from polarization data.	43
7	The electrochemical parameters and the corresponding inhibition efficiency of AA6061 in 1 M Na ₂ HPO ₄ in the absence and presence of different concentrations of polysorbate 80 at different temperatures from EIS data.	51
8	Activation thermodynamic parameters of the corrosion of AA6061 in 1 M Na ₂ HPO ₄ in the absence and presence of polysorbate 80 from polarization measurements.	52
9	Langmuir parameters of the corrosion process in the absence and presence of different concentrations of polysorbate 80 from polarization measurements at 303 K.	55
10	Flory-Huggins isotherm parameters of the corrosion process in the absence and presence of different concentrations of polysorbate 80 from polarization measurements.	58
11	The electrochemical parameters and the corresponding inhibition efficiency of AA6061 in 3.5 % NaCl in the absence and presence of different concentrations of polysorbate 80 at 303 K from polarization data.	63
12	The electrochemical parameters and the corresponding inhibition efficiency of AA6061 in 3.5 % NaCl in the absence and presence of different concentrations of polysorbate 80 at 303 K from EIS data.	67

13	Langmuir parameters of the corrosion process in the presence of polysorbate 80 from polarization measurements.	69
14	Langmuir parameters of the corrosion process in the presence of polysorbate 80 from impedance measurements.	70
15	The electrochemical parameters and the corresponding inhibition efficiency of AA6061 in 3.5 % NaCl in the absence and presence of 500 ppm of polysorbate 80 at different temperatures from polarization data.	72
16	Activation thermodynamic parameters of the corrosion process in the absence and presence of 500 ppm of polysorbate 80 from polarization measurements.	75
17	The electrochemical parameters and the corresponding inhibition efficiency of AA6061 in 3.5 % NaCl in the absence and presence of 500 ppm of polysorbate 80 at different scan rates from polarization data.	79
18	The electrochemical parameters and the corresponding inhibition efficiency of AA6061 in 1 M Na ₂ HPO ₄ in the absence and presence of different concentrations of CeCl ₃ at 303 K from polarization data.	90
19	The electrochemical parameters and the corresponding inhibition efficiency of AA6061 in 1 M Na ₂ HPO ₄ in the absence and presence of different concentrations of Ce ₂ (SO ₄) ₃ at 298 K from polarization data	90 a.
20	The Data of fitting experimental impedance spectra for AA6061 in 1 M Na ₂ HPO ₄ in the presence of different concentrations of CeCl ₃ at 298 I	95 K.
21	The Data of fitting experimental impedance spectra for AA6061 in 1M Na ₂ HPO ₄ in the presence of different concentrations of Ce ₂ (SO ₄) ₃ at 298	
22	The electrochemical parameters and the corresponding inhibition efficiency of AA6061 in 1 M Na ₂ HPO ₄ in the presence of 500 ppm of Ce ₂ (SO ₄) ₃ at different temperatures from polarization data.	.00
23	Activation thermodynamic parameters of the corrosion process for AA6061 in 1 M Na ₂ HPO ₄ in the absence and presence of Ce ₂ (SO ₄) ₃ .	100
24	The electrochemical parameters and the corresponding inhibition efficiency of AA6061 in 1 M Na ₂ HPO ₄ in the presence of 500 ppm of CeCl ₃ at different immersion times from polarization data.	.03

25	The electrochemical parameters and the corresponding inhibition efficiency of AA6061 in 1 M Na ₂ HPO ₄ in the presence of 500 ppm of Ce ₂ (SO ₄) ₃ at different immersion times from polarization data.	104
26	The electrochemical parameters and the corresponding inhibition efficiency of AA6061 in 1 M Na ₂ HPO ₄ in the presence of 500 ppm of CeCl ₃ at different scan rates at 298 K from polarization data.	106
27	The electrochemical parameters and the corresponding inhibition efficiency of AA6061 in 1 M Na_2HPO_4 in the presence of 500 ppm of $Ce_2(SO_4)_3$ at different scan rates at 303 K from polarization data.	107
28	The electrochemical parameters and the corresponding inhibition efficiency of AA6061 in 3.5 % NaCl in the absence and presence of different concentrations of CeCl ₃ at 298 K from polarization data.	111
29	The electrochemical parameters and the corresponding inhibition efficiency of AA6061 in 3.5 % NaCl in the absence and presence of different concentrations of Ce ₂ (SO ₄) ₃ at 298 K from polarization date	112 a.
30	The electrochemical parameters and the corresponding inhibition efficiency of AA6061 in 3.5 % NaCl in the absence and presence of different concentrations of CeCl ₃ at 303 K from EIS data.	117
31	The electrochemical parameters and the corresponding inhibition efficiency of 6061 AA in 3.5 % NaCl in the absence and presence of different concentrations of Ce ₂ (SO ₄) ₃ at 303 K from EIS data.	118
32	The electrochemical parameters and the corresponding inhibition efficiency of AA6061 in 2% NaCl in the absence and presence of different concentrations of CeCl ₃ at 303 K from polarization data.	121
33	The electrochemical parameters and the corresponding inhibition efficiency of AA6061 in 2% NaCl in the absence and presence of different concentrations of Ce ₂ (SO ₄) ₃ at 303K from polarization data.	122
34	The electrochemical parameters and the corresponding inhibition efficiency of AA6061 in 3.5 % NaCl in the presence of 500 ppm of CeCl ₃ at different temperatures from polarization data.	124
35	The electrochemical parameters and the corresponding inhibition efficiency of AA6061 in 3.5 % NaCl in the presence of 500 ppm of Ce ₂ (SO ₄) ₃ at different temperatures from polarization data.	125

36	The electrochemical parameters of AA6061 in 3.5% NaCl in the presence of 500 ppm of Ce ₂ (SO ₄) ₃ at 298 K from EIS data.	128
37	Chemical analysis of the monazite concentrate.	131
38	Chemical composition of sulfate solution with the leaching efficiencies of the metals of interest.	132
39	ICP chemical analysis of REE.	133
40	Effect of TBP concentration upon Ce(IV) extraction efficiency.	134
41	Effect of pH value upon Ce(IV) extraction efficiency.	135
42	Effect of shaking time upon Ce(IV) extraction efficiency.	136
43	Effect of O/A ratios upon Ce(IV) extraction efficiency.	137
44	Effect of stripping reagent type upon Ce(IV) stripping efficiency.	138
45	Effect of stripping reagent concentration upon Ce(IV) stripping efficiency.	139
46	Effect of contact time upon Ce(IV) stripping efficiency.	140
47	Effect of A/O ratios upon Ce(IV) stripping efficiency.	141
48	Effect of H ₂ O ₂ concentration with 2M H ₂ SO ₄ as stripping agent upon Ce stripping efficiency.	142
49	Effect of stripping reagent concentration upon Ce stripping efficiency.	145
50	Effect of contact time upon Ce stripping efficiency.	146
51	Effect of A/O ratios upon Ce stripping efficiency.	147
52	Effect of H ₂ O ₂ concentration with 4M HCl as stripping agent upon Ce stripping efficiency.	147

List of Figures

Figure	J	Page
1	Sketch map showing major geologic units of Egypt (Survey Dept., Cairo, 1951).	17
2	The potentiodynamic polarization curves of AA6061 in 1 M Na_2HPO_4 solution without and with different concentrations of polysorbate 80 at 303 K.	39
3	The potentiodynamic polarization curves of AA6061 in 1 M Na_2HPO_4 Solution without and with different concentrations of polysorbate 80 at 313 K.	39
4	The potentiodynamic polarization curves of AA6061 in 1 M Na_2HPO_4 solution without and with different concentrations of polysorbate 80 at 323 K.	40
5	The potentiodynamic polarization curves of AA6061 in 1 M Na_2HPO_4 solution without and with different concentrations of polysorbate 80 at 333 K.	40
6	Equivalent circuit used for modeling the impedance results.	47
7	Nyquist plots for AA6061 in 1 M Na ₂ HPO ₄ solution without and with different concentrations of polysorbate 80 at OCP and 303 K.	48
8	Nyquist plots for AA6061 in 1 M Na ₂ HPO ₄ solution without and with different concentrations of polysorbate 80 at OCP and 313 K.	48
9	Nyquist plots for AA6061 in 1 M Na ₂ HPO ₄ solution without and with different concentrations of polysorbate 80 at OCP and 323 K.	49
10	Nyquist plots for AA6061 in 1 M Na ₂ HPO ₄ solution without and with different concentrations of polysorbate 80 at OCP and 333 K.	49
11	Bode plots for AA6061 in 1 M Na ₂ HPO ₄ solution without and with different concentrations of polysorbate 80 at OCP and 303 K.	50
12	Arrhenius plots for AA6061 in 1.0 M Na ₂ HPO ₄ in the absence and presence of 500 ppm polysorbate 80 from polarization measurements.	53

13	Eyring plot for AA6061 in 1.0 M Na ₂ HPO ₄ in the absence and presence of 500 ppm polysorbate 80 from polarization measurements.	53
14	Curve fitting of the corrosion data of AA6061 in 1.0 M Na ₂ HPO ₄ solution in the presence of different concentrations of polysorbate 80 at 303 K to Langmuir isotherm from polarization measurements.	55
15	Curve fitting of the corrosion data of AA6061 in 1.0 M Na ₂ HPO ₄ solution in the presence of different concentrations of polysorbate 80 at 303 K to Flory-Huggins isotherm from polarization measurements.	57
16	The cyclic potentiodynamic polarization curves of AA6061 in 3.5 % NaCl solution in absence and presence of 500 ppm of polysorbate 80 at 303 K.	60
17	potentiodynamic polarization curves of AA6061 in 3.5 % NaCl solution without and with different concentrations of polysorbate 80 at 303 K.	63
18	E_{pit} for AA6061 in 3.5 % NaCl solution with different concentrations of polysorbate 80 at 303 K.	64
19	Nyquist plots for AA6061 in 3.5 % NaCl solution without and with different concentrations of polysorbate 80 at 303 K.	66
20	Bode plots for AA6061 in 3.5 % NaCl solution without and with different concentrations of polysorbate 80 at 303 K.	66
21	Curve fitting of the corrosion data of AA6061 in 3.5 % NaCl solution in the presence of polysorbate 80 at 303 K to Langmuir isotherm from polarization measurements.	69
22	Curve fitting of the corrosion data of AA6061 in 3.5 % NaCl solution in the presence of polysorbate 80 at 303 K to Langmuir isotherm from impedance measurements.	70
23	The potentiodynamic polarization curves of AA6061 in 3.5 % NaCl solution at different temperatures.	72
24	The potentiodynamic polarization curves of AA6061 in 3.5 % NaCl solution with 500 ppm of polysorbate 80 at different temperatures.	73
25	E _{pit} for AA6061 in 3.5 % NaCl solution with 500 ppm of	74

polysorbate 80 at different temperatures.

Eyring plot for AA6061 in 3.5 % NaCl in the absence and 500 ppm polysorbate 80 from polarization measurements.	presence of	76
The potentiodynamic polarization curves of AA6061 in 3.5 solution at different scan rates.	5 % NaCl	78
The potentiodynamic polarization curves of AA6061 in 3.5 solution with 500 ppm of polysorbate 80 at different scan ra		78
Relation between I_{pass} and U $^{1/2}$ at potential -1000 mV from measurements for blank and inhibited solution.	polarization	79
Some Current / Time transients of AA6061 in 3.5 % NaCl at different anodic potentials (-800 & -685 & -660 mV).	solution	82
Current / Time transients of AA6061 in 3.5 % NaCl solution presence of 500 ppm of polysorbate 80 at different potential (-800 & -685 & -660 mV).		83
The Current / Time transients of AA6061 in 3.5 % NaCl so with different concentrations of polysorbate 80 at 303 K and		84
Current / Time curves of 6061 AA in 3.5 % NaCl solution 500 ppm of polysorbate 80 at different temperatures and -68		85
Relation between (1/t _i) vs potential for blank and inhibited	solution.	86
potentiodynamic polarization curves of AA6061 in 1 M Na solution without and with different concentrations of CeCl ₃		89
potentiodynamic polarization curves of AA6061 in 1 M Na solution without and with different concentrations of Ce ₂ (Se		89
Equivalent circuit used for modeling the impedance results from inhibited solutions.	obtained	94
Nyquist plots for AA6061 in 1 M Na ₂ HPO ₄ solution without different concentrations of CeCl ₃ at 298 K.	ut and with	95
Nyquist plots for AA6061 in 1 M Na ₂ HPO ₄ solution without	ut and with	96

	different concentrations of Ce ₂ (SO ₄) ₃ at 298 K.	
41	Bode plots for AA6061 in 1 M Na ₂ HPO ₄ solution with different concentrations of CeCl ₃ at 298 K.	97
42	Bode plots for AA6061 in 1 M Na ₂ HPO ₄ solution with different concentrations of Ce ₂ (SO ₄) ₃ at 298 K.	97
43	The potentiodynamic polarization curves of AA6061 in 1 M Na ₂ HPO ₄ solution with 500 ppm of Ce ₂ (SO ₄) ₃ at different temperatures	99
44	Arrhenius plots for AA6061 in 1.0 M Na ₂ HPO ₄ in the absence and presence of 500 ppm Ce ₂ (SO ₄) ₃ from polarization data.	100
45	Transition state plots for AA6061 in 1M Na ₂ HPO ₄ in the absence and presence of 500 ppm Ce ₂ (SO ₄) ₃ from polarization data.	101
46	The potentiodynamic polarization curves of AA6061 in 1 M Na ₂ HPO ₄ solution with 500 ppm of CeCl ₃ at different immersion times at 298 K.	
47	The potentiodynamic polarization curves of AA6061 in 1 M Na_2HPO_4 solution with 500 ppm of $Ce_2(SO_4)_3$ at different immersion times at 303 K.	104
48	The potentiodynamic polarization curves of 6061 AA in 1 M Na ₂ HPO ₄ solution with 500 ppm of CeCl ₃ at different scan rates at 298	106 3 K.
49	The potentiodynamic polarization curves of 6061 AA in 1 M Na ₂ HPO ₄ solution with 500 ppm of Ce ₂ (SO ₄) ₃ at different scan rates at 303 K.	107
50	The potentiodynamic polarization curves of AA6061 in 3.5% NaCl solution without and with different concentrations of CeCl ₃ at 298 K.	111
51	The potentiodynamic polarization curves of AA6061 in 3.5 % NaCl solution without and with different concentrations of Ce ₂ (SO ₄) ₃ at 298 l	112 K.
52	The cyclic potentiodynamic polarization curves of AA6061 in 3.5 % NaCl solution in absence and presence of 500 ppm of Ce ₂ (SO ₄) ₃ at 5 mVs ⁻¹ and 298 K.	114
53	Nyquist plots for AA6061 in 3.5 % NaCl solution without and with different concentrations of CeCl ₃ at 303 K.	117
54	The electrochemical parameters and the corresponding inhibition	118

	efficiency of 6061 AA in 3.5 % NaClin the absence and presence of different concentrations of Ce ₂ (SO ₄) ₃ at 303 K from EIS data.	
55	Bode plots for AA6061 in sea water solution without and with different concentrations of CeCl ₃ at 303 K.	119
56	Bode plots for AA6061 in 3.5 % NaCl solution without and with different concentrations of Ce ₂ (SO ₄) ₃ at 303 K.	119
57	The potentiodynamic polarization curves of AA6061 in 2% NaCl solution without and with different concentrations of CeCl ₃ at 303K.	121
58	The potentiodynamic polarization curves of AA6061 in 2% NaCl solution without and with different concentrations of Ce ₂ (SO ₄) ₃ at 303	122 K.
59	The potentiodynamic polarization curves of AA6061 in 3.5 % NaCl solution with 500 ppm of CeCl ₃ at different temperatures.	124
60	The potentiodynamic polarization curves of AA6061 in 3.5 % NaCl solution with 500 ppm of Ce ₂ (SO ₄) ₃ at different temperatures.	125
61	Arrhenius plots for AA6061 in 3.5% NaCl in the absence and presence of 500 ppm CeCl ₃ from polarization measurements.	126
62	Arrhenius plots for AA6061 in 3.5% NaCl in the absence and presence of 500 ppm Ce ₂ (SO ₄) ₃ from polarization data.	126
63	Nyquist plots for AA6061 in 3.5% NaCl solution with 500 ppm of Ce ₂ (SO ₄) ₃ at 298 K at different immersion times.	128
64	Bode plots for AA6061 in 3.5% NaCl solution with 500 ppm of Ce ₂ (SO ₄) ₃ at 298 K at different immersion times.	129
65	The potentiodynamic polarization curves of AA6061 in 3.5% NaCl solution with 500 ppm of Ce ₂ (SO ₄) ₃ at 298 K with different pH.	130
66	(a) SEM image recorded for pure AA6061.(b) EDX analysis for pure AA6061.	131
67	(a) SEM image recorded for AA6061 in 3.5% NaCl.(b) EDX analysis for AA6061 in 3.5% NaCl.	132
68	(a) SEM image recorded for AA6061 in 3.5% NaCl with 500 ppm of Polysorbate 80 .	132
80.	(b) EDX analysis for AA6061 in 3.5% NaCl with 500 ppm of Polyso	rbate